

# Raman Spectroscopic Studies of Model Human Pulmonary Surfactant Systems: Phospholipid Interactions with Peptide Paradigms for the Surfactant Protein SP-B<sup>†</sup>

James S. Vincent,<sup>‡</sup> Susan D. Revak,<sup>§</sup> Charles G. Cochrane,<sup>§</sup> and Ira W. Levin<sup>\*||</sup>

*Chemistry Department, University of Maryland Baltimore County, 5401 Wilkens Avenue, Catonsville, Maryland 21228, Department of Immunology, Research Institute of Scripps Clinic, La Jolla, California 92037, and Laboratory of Chemical Physics, National Institute of Diabetes and Digestive and Kidney Diseases, National Institutes of Health, Bethesda, Maryland 20892*

*Received April 26, 1991; Revised Manuscript Received June 14, 1991*

**ABSTRACT:** The temperature dependence of dipalmitoylphosphatidylcholine (DPPC)/phosphatidylglycerol (PG) multilayers, reconstituted with various synthetic peptides for modeling human lung surfactant, was monitored by vibrational Raman spectroscopy. The synthetic peptides consisted, respectively, of residues 59–81 of the human surfactant protein SP-B and 21 amino acid residue peptides containing repeating units of arginine separated by either four or eight leucines (RL<sub>4</sub> or RL<sub>8</sub>). Each peptide demonstrated the ability to reduce significantly the surface tension of analogues of the phospholipid mixture used in the Raman studies. Raman spectroscopic integrated band intensities and relative peak height intensity ratios, two spectral parameters used to determine bilayer disorder, provided sensitive probes for characterizing multilayer perturbations in the reconstituted liposomes. Temperature profiles derived from the various Raman intensity parameters for the 3100–2800-cm<sup>-1</sup> carbon–hydrogen (C–H) stretching mode region, a spectral interval representative of acyl chain vibrations, reflected lipid reorganizations due to the bilayer interactions of these peptides. For the three reconstituted multilamellar surfactant systems, the gel-to-liquid-crystalline phase-transition temperatures *T<sub>m</sub>*, defined by acyl chain C–H stretching mode order/disorder parameters, increased from 35 °C in the peptide free system to 37–38 °C, indicating increased lipid headgroup constraints for the model liposomes. Although the values of *T<sub>m</sub>* were similar for the three recombinant lipid/peptide assemblies, individual phase-transition cooperativities varied significantly between systems and between spectroscopically derived order/disorder parameters.

**P**ulmonary surfactant, consisting of a mixture of phospholipids and associated proteins that coat the lung alveoli, forms an air–water barrier that prevents alveolar collapse and lung edema (Clements, 1977). Surfactant, produced by type II pneumocyte cells, is stored until required in tubular myelin structures in the alveolar lining just below the air–hypophase boundary (Scarpelli, 1988). By lowering the surface tension of the alveolar lining, surfactant materials permit an expansion of the lung during the inspiration of air, while providing alveolar stability during exhalation. Although the primary lipid constituents of the surfactant layer are dipalmitoylphosphatidylcholine (DPPC)<sup>1</sup> and phosphatidylglycerol (PG) (Harwood & Richards, 1985), proteins comprise approximately 1–5% by weight of lung surfactant, with the major component of the system being the *M*<sub>r</sub> 35 000 SP-A protein (King et al., 1973). Proteins ranging from *M*<sub>r</sub> 9000 to 70 000 have also been isolated (Phizackerley et al., 1979; Suzuki et al., 1986; Takahashi & Fujiwara, 1986; Whitsett et al., 1986; Hawgood et al., 1987; Harwood & Richards, 1985).

In human surfactant material, recent attention has focused on the SP-B protein, which exists as a dimeric species with an *M*<sub>r</sub> of 18 000. The importance of this protein is demonstrated in its ability to affect surface tension properties. In particular, the addition of 1% SP-B to a phospholipid mixture dramatically reduces the liposomal surface tension to one-seventh of the value obtained for the pure phospholipid (Revak

et al., 1988). The primary structure of SP-B is significant, since it exhibits alternating regions of hydrophobic residues separated by hydrophilic residues (Revak et al., 1988; Hawgood et al., 1987; Glasser et al., 1987; Jacobs et al., 1987; Warr et al., 1987). Portions of the SP-B protein may form amphipathic helices with excess positive charge on the hydrophilic sides. This general amphipathic topology, in which the hydrophilic areas are positively charged, has prompted studies demonstrating that arrays of hydrophobic amino acids (leucines) with intermittent positively charged hydrophilic residues (arginines or lysines) provide suitable substitutes for SP-B in reconstituted surfactant systems (Cochrane & Revak, 1990; and unpublished observations). As part of a general program concerned with the design of effective surfactant materials, we synthesized for physical and spectroscopic characterization peptides containing 21 amino acid residues in which arginines are separated by either four or eight leucines, that is, peptides composed of RL<sub>4</sub> or RL<sub>8</sub> groupings and their fractions, respectively. In the present work, we report our vibrational Raman spectroscopic investigations exploring the various lipid/peptide interactions of the repetitive RL<sub>4</sub> and RL<sub>8</sub> sequences, as well as the 59–81 amino acid fragment of SP-B, which have been reconstituted in dipalmitoylphosphatidylcholine (DPPC)/phosphatidylglycerol (PG) lipid bilayer assemblies.

Vibrational Raman spectroscopy represents a sensitive noninvasive technique for studying the thermotropic behavior

<sup>†</sup> C.G.C. and S.D.R. acknowledge support from USPH Grant HL 23584 and ONR Grant N00014-91-J-1158.

<sup>‡</sup> University of Maryland Baltimore County.

<sup>§</sup> Research Institute of Scripps Clinic.

<sup>||</sup> NIDDK, NIH.

<sup>1</sup> Abbreviations: DPPC, dipalmitoylphosphatidylcholine; PG, phosphatidylglycerol (from egg lecithin); POPG, 1-palmitoyl-2-oleoylphosphatidylglycerol; SP, surfactant protein.

of lipid membrane systems. In applying Raman spectroscopy to the reconstituted bilayer systems described above, we emphasize the temperature dependence of several spectral peak height intensity ratios and integrated intensity parameters determined from the lipid acyl chain methylene and methyl C-H stretching modes. These derived parameters reflect the inter- and intrachain order characteristic of the reconstituted bilayer assemblies (Levin, 1984, 1985). For example, the spectral carbon-hydrogen (C-H) intensity ratio,  $I_{2850}/I_{2880}$ , where the 2850- and 2880- $\text{cm}^{-1}$  modes refer to the acyl chain methylene ( $\text{CH}_2$ ) symmetric and asymmetric stretching vibrations, respectively, reflects the lateral chain-chain interactions defining the bilayer dynamics. Order/disorder measures also arising from chain-chain interactions, but with contributions from intrachain trans/gauche isomerizations, are determined from the  $I_{2935}/I_{2880}$  intensity parameter. The 2935- $\text{cm}^{-1}$  feature represents a complex spectral interval that contains spectral components from Fermi resonance interactions involving the chain methylene moieties and, separately, the C-H symmetric stretching modes of the chain methyl termini of the lipids comprising the liposomes (Hill & Levin, 1979). Although no Raman studies of surfactant material have appeared, to our knowledge, in the literature, several vibrational infrared spectroscopic investigations of various lung surfactant systems have, however, been reported previously. For example, Mautone et al. (1987), using Fourier transform infrared spectroscopy, studied the effect of calcium ions on the thermotropic properties of whole protein extracts from rabbit lung surfactant. In addition, Reilly et al. (1989) and Dluhy et al. (1989) used infrared spectroscopic techniques to investigate the properties of model surfactant systems in which SP-A was the associated protein in the reconstituted systems.

#### MATERIALS AND METHODS

Synthetic L- $\alpha$ -dipalmitoylphosphatidylcholine (DPPC) and isolated egg phosphatidylglycerol (PG) were obtained from Avanti Polar Lipids and used without further purification. The multilayer dispersions of the 3:1 weight ratio mixture of DPPC and PG were prepared according to previous studies (Revak et al., 1988, 1991) by first dissolving the lipids in a mixture of chloroform and methanol and evaporating the solvent under a nitrogen flow and finally under high vacuum. Water is added to disperse the lipid, and the mixture is incubated, accompanied by gentle mixing, for an hour at 43 °C in the liquid-crystalline phase. A saline solution is added to restore isotonicity, and the resulting dispersion is subjected to three freeze-thaw cycles through the phase transition. After the samples were sealed in glass capillary tubes, the multilayers were compacted in a hematocrit centrifuge. In cases where the lipid samples were gelatinous and did not compact easily, the dispersions were centrifuged in a Beckmann Ultracentrifuge for 20 min at 80000g. Samples were stored in a refrigerator at 2–5 °C for at least 24 h before recording the spectra.

Synthetic peptides were synthesized following the methods of Merrifield (1963) as described previously (Revak et al., 1991). These specific peptide sequences include RL<sub>4</sub> (RLLLRLLLRLLLRLLLR), RL<sub>8</sub> (RLLLLLLRLLLLLLRLLL), and the residues 59–81 of SP-B (DTLLGRMLPQLVCRVLRCMDD), where the capital letters represent the standard symbols for the specific amino acids.

Peptide/lipid multilayers (10% weight peptide/weight lipid) were reconstituted by adding 2 mg of peptide to 20 mg of a lipid mixture of DPPC and PG in the chloroform/methanol solvent mixture. (The approximate mole ratio of lipid to peptide for the three systems is 40:1.) After the solvent was

evaporated under a stream of nitrogen at 40 °C, final traces of solvent were removed, as before, under vacuum. The composition of the egg PG acyl chains is about 35% palmitoyl, 31% oleoyl, 17% linoleoyl, and 12% stearoyl. Human lung surfactant phospholipids have about 15% unsaturated acyl chains, an amount that approximates the unsaturation contribution of the PG chains to the reconstituted surfactant. Subsequent treatment for preparing the peptide/lipid dispersions followed the same procedure described above.

Biophysical surfactant activity of the peptide/lipid vesicles was determined by using a pulsating bubble surfactometer (Revak, 1986; Enhorning, 1977). This instrument allows one to measure the ability of a sample to lower surface tension at an air/liquid interface. Samples were diluted to a concentration of 4 mg/mL phospholipid for testing. Lipid samples were reconstituted with DPPC and either egg PG or 1-palmitoyl-2-oleoylphosphatidylglycerol (POPG) to form the 3:1 mixed phospholipid. The surfactant activity of the peptide/lipid vesicles derived from either the PG or POPG mixed lipid was nearly identical.

Raman spectra were observed as a function of temperature at 1.0 °C intervals from approximately 5 to 55 °C. The specific temperature range varied between experiments. A thermostated bath circulated heat-exchanged fluid through a thermoelectrically controlled sample holder, which also housed the thermocouple used for monitoring the bath temperature. A separate solid-state temperature-sensitive device controlled the power supplied to the thermoelectric temperature regulator. Laser excitation at 514.5 nm, obtained from a Spectra Physics 165 Argon unit, ranged from 30 to 75 MW for the various experiments. The scattered light was collected with a Spex Triplemate spectrograph at a spectral resolution of  $\sim 5\text{--}6\text{ cm}^{-1}$  for the 1200 line/mm grating that was used to span the 3100–2800- $\text{cm}^{-1}$  region. Spectra were detected with an EG&G thermoelectrically cooled intensified silicon diode array. Raman emission, as well as temperature bath control, were recorded and controlled, respectively, with a DEC PDP 11/23 based laboratory computer system. Spectral files were transferred to a DEC PDP 11/84 computer for both data storage and spectral manipulation.

Since the lipid/peptide mole ratios of the reconstituted systems are of the order of 40:1, no protein spectral subtractions were required in order to determine pure lipid C-H stretching mode region spectra. Examination of the lipid/protein spectra demonstrated that protein subtractions were unnecessary.

#### RESULTS

##### *Biophysical Activity of Lipid/Peptide Mixtures*

To determine whether the lipid/peptide mixtures had the biophysical activity associated with surfactants, the mixtures were analyzed for their ability to lower surface tension in a pulsating bubble surfactometer. Phospholipid plus SP-B peptide 59–81, RL<sub>4</sub>, or RL<sub>8</sub> all show a significant decrease in surface tension over that obtained with the phospholipid alone. Figure 1 displays the data for a phospholipid mixture composed of 3:1 weight ratio DPPC/POPG combined with the surfactant peptides. Data for the 3:1 weight ratio DPPC/PG phospholipid mixture is nearly identical with that of Figure 1.

##### *Raman Spectral Studies*

**Phospholipid Mixture 3:1 DPPC/PG.** Although the 3100–2800- $\text{cm}^{-1}$  C-H stretching mode region is quite complex, changes in the spectral intensities of these vibrations as a

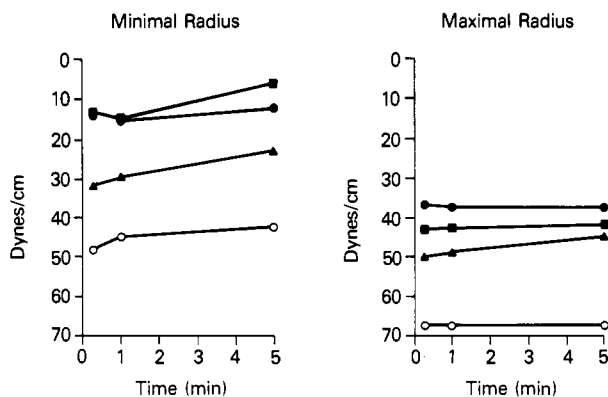


FIGURE 1: Surface tension (dynes/cm) calculated from pressure gradients at the minimal and maximal radii of the pulsating bubble. Pulsation of 20 cycles/min started 10 s after bubble formation. Peptides (10% by weight) were added to phospholipids (PL, DPPC/POPG, 3:1). Samples are PL +  $RL_8$  (■), PL +  $RL_4$  (●), PL + SP-B peptide 59–81 (▲), and PL alone (○).

function of bilayer perturbation and temperature reflect both inter- and intramolecular changes within the hydrophobic region of the membrane (Hill & Levin, 1979; Levin, 1984). Figure 2a presents a topological plot of the C–H stretching mode region for the lipid multilayers derived from the 3:1

DPPC/PG phospholipid mixture. The axes in the plane are the wave number and temperature, while the intensity of the Raman scattering is graphed on the out-of-plane axis. As shown in this figure and the curve in Figure 2b, curve C, the integrated intensity corresponding to this spectral interval first increases gradually with temperature, reaching a maximum at approximately 20 °C, and then decreases in intensity until the limit of the temperature scan is reached. This integrated intensity parameter represents a function of the number of molecule scatterers in the exciting laser beam and the polarizability changes of the molecules induced by the various vibrational displacement coordinates. (Since the 3000- $cm^{-1}$  spectral region represents a complex manifold of vibrational levels, we find it useful to monitor the relative total integrated intensity of the Raman emission over the entire 2800–3100- $cm^{-1}$  interval, rather than to attempt spectral deconvolutions and individual band integrations.) The intensity maximum shown in Figure 2a and Figure 2b, curve C, around 20–24 °C suggests a bilayer rearrangement to a more ordered lattice in this temperature regime, perhaps a lipid reorganization involving domain formation or lateral segregation of the two lipid species. The subsequent decrease in the integrated intensity parameter (Figure 2b, curve C) correlates with decreasing bilayer order and lattice expansion and also spans the gel-to-liquid-crystalline phase transition as determined by both

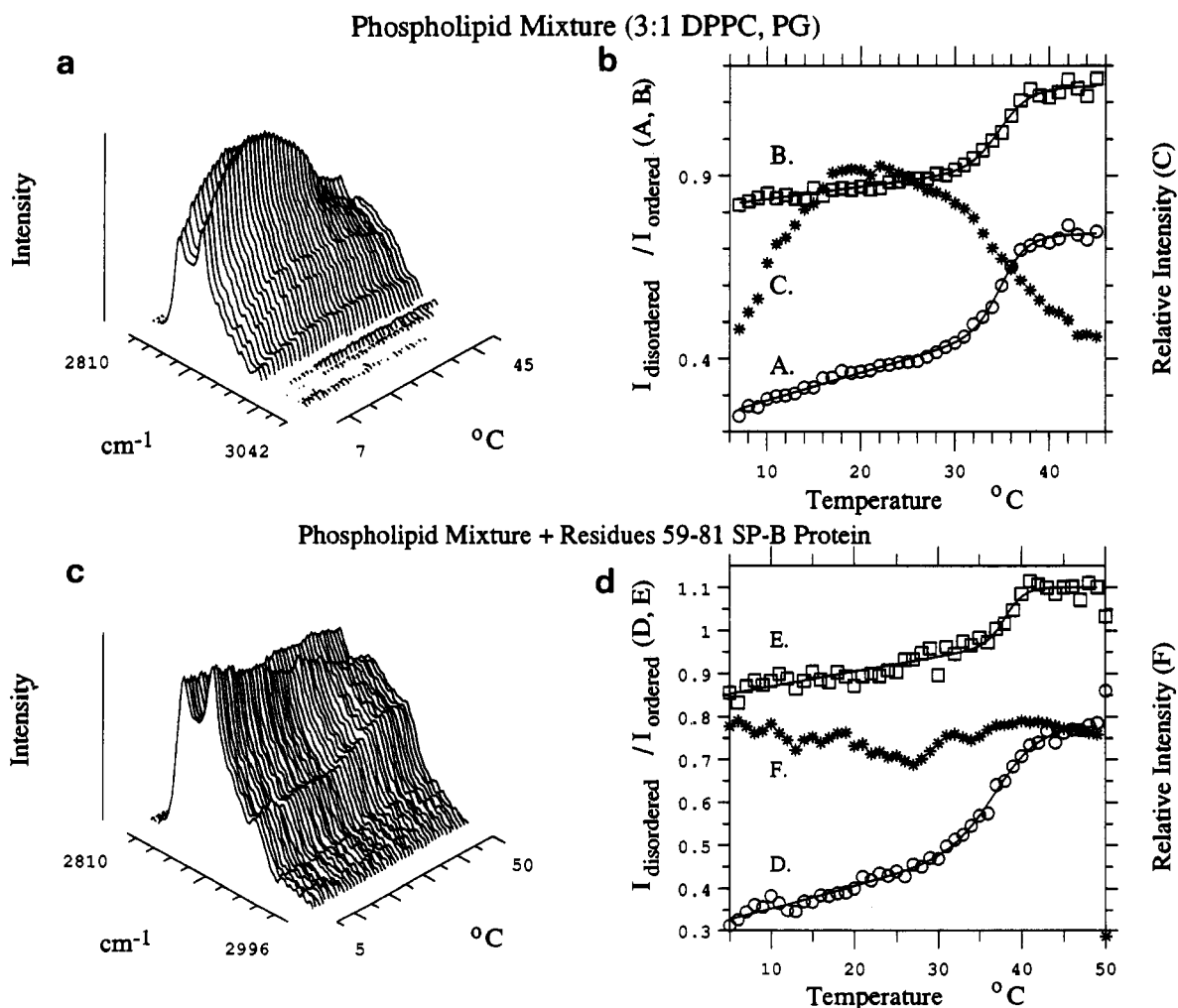


FIGURE 2: Raman spectra of the CH stretching mode region (2800–3000  $cm^{-1}$ ) as a function of temperature. (a) Phospholipid mixture (3:1) of DPPC and PG. (b) Peak height intensity ratios of the sample of Figure 2a; (A)  $I_{2935}/I_{2880}$ ; (B)  $I_{2850}/I_{2880}$ ; and (C) the relative integrated intensity over the CH stretching mode region. (c) Phospholipid mixture (3:1) of DPPC and PG with residues 59–81 of the SP-B peptide. (d) Peak height intensity ratios of the sample of Figure 2c; (D)  $I_{2935}/I_{2880}$ ; (E)  $I_{2850}/I_{2880}$ ; and (F) the relative integrated intensity over the CH stretching mode region. The lines were calculated by using a two-state model for lipid transitions to fit the experimental points in A, B, D, and E.

Table I: Raman Spectral Parameters for Multilamellar Vesicles Composed of a 3:1 Weight Ratio Dipalmitoylphosphatidylcholine (DPPC) and Phosphatidylglycerol (PG) Mixture Reconstituted with the Synthetic Peptides, Residues 59–81 of SP-B, RL<sub>4</sub>, and RL<sub>8</sub>

sample	peak height intensity ratios <sup>a</sup>							
	$I_{2935}/I_{2880}$				$I_{2850}/I_{2880}$			
	gel state	liq cryst	$T_m$ (°C) <sup>b</sup>	$\Delta T$ (°C) <sup>b</sup>	gel state	liq cryst	$T_m$ (°C)	$\Delta T$ (°C)
pure DPPC	0.46	0.83	41.3 ± 0.2	0.9 ± 0.1	0.78	0.95	41.4 ± 0.2	1.1 ± 0.1
DPPC/PG mixture	0.36	0.74	35.0 ± 0.3	5.5 ± 0.8	0.87	1.15	34.9 ± 0.5	6.4 ± 1.1
mixture + SP-B <sup>c</sup>	0.42	0.78	37.4 ± 0.3	10.8 ± 1.0	0.91	1.10	38.2 ± 0.4	4.6 ± 1.4
mixture + RL <sub>4</sub> <sup>d</sup>	0.40	0.75	37.8 ± 0.5	8.0 ± 1.5	0.79	1.06	36.9 ± 0.3	3.5 ± 1.0
mixture + RL <sub>8</sub> <sup>d</sup>	0.38	0.69	37.0 ± 0.5	12.0 ± 2.5	0.80	1.00	37.8 ± 1.0	15.0 ± 3.5

<sup>a</sup> The peak height intensity ratios for the gel and liquid-crystalline states were taken 15 °C below and above the phase-transition temperature  $T_m$ , respectively. The uncertainties of the reported peak height intensity ratios are ±0.02. <sup>b</sup> The main phase-transition temperatures  $T_m$  and the width of the phase transition  $\Delta T$  were determined by fitting a theoretical line derived from a two-state model for lipid phase transitions (Kirchhoff & Levin, 1987) to the peak height ratio data. <sup>c</sup> Residues 59–81 of SP-B. <sup>d</sup> 21 amino acid polypeptide.

peak height intensity ratios,  $I_{2935}/I_{2880}$  and  $I_{2850}/I_{2880}$ , displayed by the temperature profiles in Figure 2b, curves A and B. The peak intensity ratios of the 2935-cm<sup>-1</sup> and the 2880-cm<sup>-1</sup> features,  $I_{2935}/I_{2880}$ , displayed in Figure 2b, curve A, increase toward greater bilayer disorder with rising temperature. The abrupt change in the sigmoidal curve at 35.0 °C is indicative of the gel-to-liquid-crystalline phase transition. This spectral parameter reflects primarily interchain bilayer disorder with some contributions from intrachain trans/gauche isomerization. The peak height intensity ratio parameter,  $I_{2850}/I_{2880}$ , reflecting pure lateral chain-chain interactions, increases with temperature, as shown in Figure 2b, curve B, in the same manner as the  $I_{2935}/I_{2880}$  parameter and yields essentially the same  $T_m$ . Values of  $T_m$  and the phase-transition widths  $\Delta T$  were determined by fitting a two-state model to the temperature profiles (Kirchhoff & Levin, 1987) and are summarized in Table I for the 3:1 phospholipid mixture and for pure DPPC bilayers for comparison purposes. The analysis of the Raman data assumes that the spectral feature (intensity ratio in this case) depends upon the distribution between two states of the observed molecules and is given by

$$\frac{I_1}{I_2} = \frac{A + a(T - T_m)}{(1 + e^t)} + \frac{B + b(T - T_m)}{(1 + e^{-t})}$$

in which  $t = (T - T_m)/D$  and  $A$ ,  $B$ ,  $a$ ,  $b$ ,  $D$ , and  $T_m$  are fit by a least-squares criterion to the data. The width of the transition  $\Delta T = 4D$ , and the phase-transition temperature is  $T_m$ . With the existing quality of data and density of points, the estimated errors in  $T_m$  are less than 0.5 °C.

As judged by the values of the  $I_{2935}/I_{2880}$  peak height intensity ratio listed in Table I, the lipid mixture exhibits a greater acyl chain order in both the gel and liquid-crystalline phases than saturated chain DPPC bilayers. However, the  $I_{2850}/I_{2880}$  ratio, reflecting solely interchain interactions, displays values implying greater disorder for the gel and liquid-crystalline phases of the DPPC/PG mixture than the pure DPPC bilayer. The increase in order shown by the  $I_{2935}/I_{2880}$  probably originates from the local rigidity induced in the middle of adjacent saturated chains by the 9,10- and 12,13-cis double bonds in the oleoyl and linoleoyl unsaturated chains of PG (Seelig & Seelig, 1977; Lavalie & Levin, 1980). The lower  $T_m$  for the lipid mixture reflects the ~40% decrease in the barriers to rotation of the methylene units adjacent to the double bond moieties (Flory, 1969) and the consequent instabilities conferred upon the bilayer as the temperature of the assembly increases. The increase in the DPPC/PG gel and liquid-crystalline phase  $I_{2850}/I_{2880}$  parameters relative to the reference DPPC bilayer system suggests a distorted acyl chain lattice structure arising from the heterogeneous packing characteristics dictated by the disparity in headgroup configurations and electrostatics for the two species in the lipid

mixture. The  $T_m$  value derived for lipid mixture is identical for the two spectral ratio indicators, illustrating high correlation between these two order/disorder parameters; that is, the lattice expansion and acyl chain trans/gauche isomerization processes occur concurrently.

**DPPC/PG Phospholipid Complex with SP-B Peptide (Residues 59–81).** The Raman spectra of the 3:1 DPPC/PG weight ratio phospholipid mixture with 10% (w/w) of the SP-B peptide over the 5–50 °C temperature range are displayed in Figure 2c. The peak height intensity ratios  $I_{2935}/I_{2880}$ , and  $I_{2850}/I_{2880}$ , curves D and E in Figure 2d, show increased  $T_m$ 's and quite different transition widths,  $\Delta T$ , in comparison with the peptide-free bilayer system. The lateral chain-chain disorder parameter,  $I_{2850}/I_{2880}$ , initially exhibits a slightly more disordered gel-phase value than the pure system but achieves a slightly more ordered liquid-crystalline phase than the peptide-free liposome. The temperature profile derived from these parameters yields a  $T_m$  of 38.2 ± 0.4 °C with a phase-transition width of  $\Delta T = 4.6 ± 1.4$  °C, the latter of which is within the error limits of the two-state statistical fit for the transition width of the DPPC/PG bilayer ( $\Delta T = 6.4 ± 1.1$  °C). The temperature dependence of the intermolecular disorder parameter with gauche/trans character,  $I_{2935}/I_{2880}$ , shows a  $T_m$  of 37.4 ± 0.3 °C but with a significantly greater width,  $\Delta T$ , of 10.8 ± 1.0 °C. The relative integrated intensity value (Figure 2d, curve F) remains nearly constant over the temperature range of 5–50 °C, in distinct contrast to the intensity curve of the phospholipid mixture devoid of peptide (Figure 2b, curve C). A summary of the spectral and thermal parameters for the binary phospholipid mixture and the ternary mixtures with either the SP-B fragment or the RL<sub>4</sub>- or RL<sub>8</sub>-based polypeptides are listed in Table I. The changes in the widths of the phase-transition regions reflect the cooperativities of the melting process. Thus, relative to the pure DPPC/PG lipid bilayer,  $\Delta T$  derived from the  $I_{2850}/I_{2880}$  parameter indicates about the same order of cooperativity for the melting process of the SP-B recombinant. The value for  $\Delta T$  determined from the  $I_{2935}/I_{2880}$  profile demonstrates that the SP-B fragment significantly decreases the cooperativity of the phase transition. We note again that gauche/trans conformational changes are sensed in some degree by the latter order/disorder parameter.

**Phospholipid Complex with either RL<sub>4</sub> or RL<sub>8</sub>.** Figure 3 displays, as a function of temperature, the peak height intensity ratios and the integrated intensity parameter over the C–H stretching mode region for the phospholipid bilayers reconstituted separately with the RL<sub>4</sub> or RL<sub>8</sub> polypeptides. The integrated intensity curves of both the RL<sub>4</sub> and RL<sub>8</sub> systems (Figure 3b, curve C and Figure 3d, curve F) first increase with temperature and after reaching a maximum around 24 °C then decrease, as expected, over the 32–42 °C temperature range

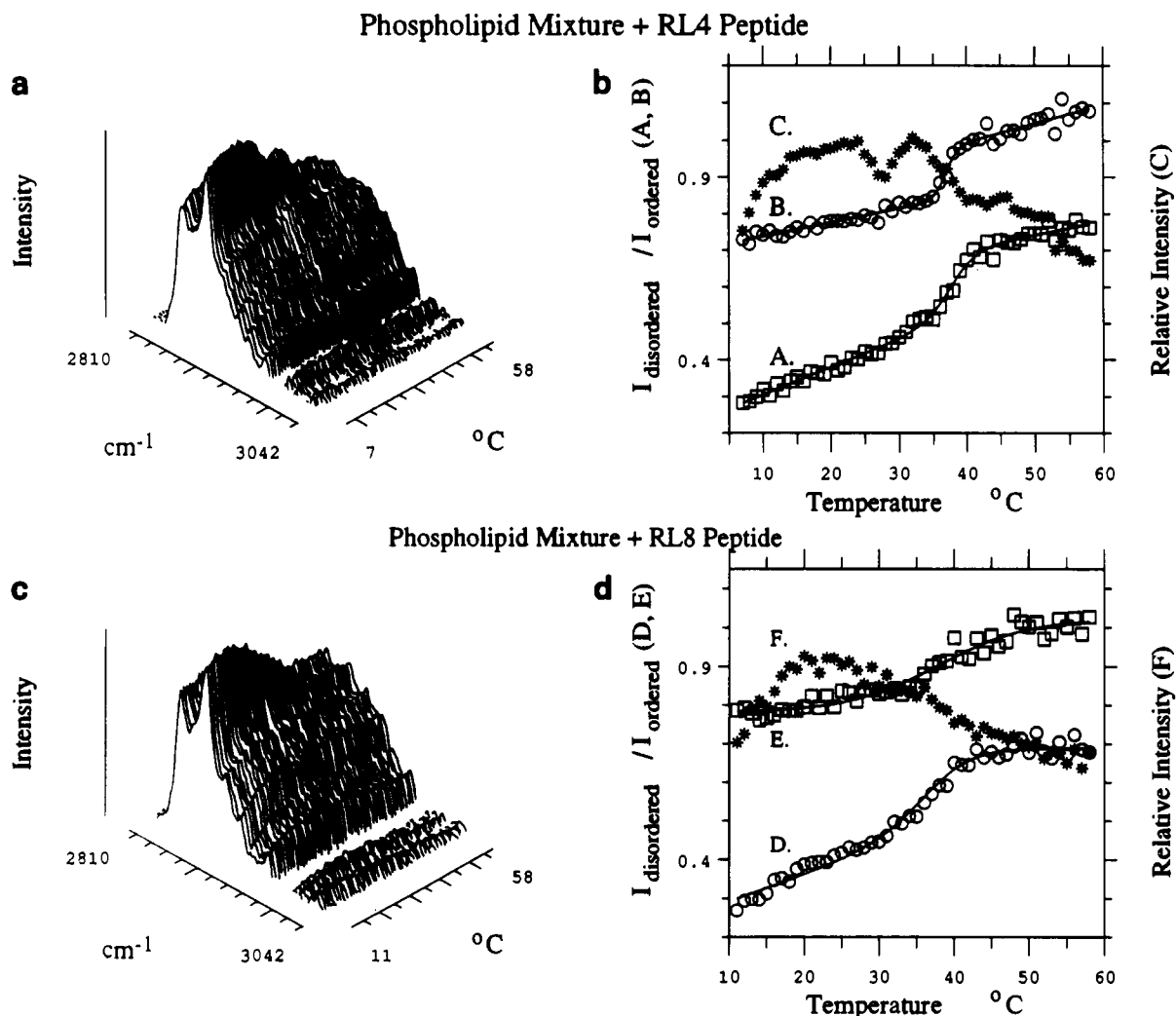


FIGURE 3: Raman spectra of the CH stretching mode region (2800–3000  $\text{cm}^{-1}$ ) as a function of temperature. (a) Phospholipid mixture (3:1) of DPPC and PG with RL<sub>4</sub>. (b) Peak height intensity ratios of the sample of Figure 3a; (A)  $I_{2935}/I_{2880}$ ; (B)  $I_{2850}/I_{2880}$ ; and (C) the relative integrated intensity over the CH stretching mode region. (c) Phospholipid mixture (3:1) of DPPC and PG with RL<sub>8</sub>. (d) Peak height intensity ratios of the sample of Figure 3c; (D)  $I_{2935}/I_{2880}$ ; (E)  $I_{2850}/I_{2880}$ ; and (F) the relative integrated intensity over the CH stretching mode region. The lines were calculated by using a two-state theory to fit the experimental points in A, B, D, and E.

of the gel-to-liquid-crystalline transition. That is, the lateral bilayer expansion for the liquid-crystalline phase leads to a reduction in the band intensity for the C–H stretching region modes. Although the general behavior of the integrated intensity is similar to that of the phospholipid mixture devoid of peptides, the overall relative intensity changes are smaller for the peptide-containing systems. When the relative intensity of each system is normalized to the integrated intensity maximum at about 20–25 °C, the peptide-free system intensity variation with temperature is about twice that of the peptide ternary complexes, suggesting that the presence of the peptide modifies bilayer structural characteristics.

As in the bilayer recombinants containing the SP-B protein fragments, the phase-transition temperatures  $T_m$  determined by the  $I_{2850}/I_{2880}$  ratio for the RL<sub>4</sub> and RL<sub>8</sub> ternary mixtures are, respectively,  $36.9 \pm 0.3$  °C and  $37.8 \pm 1.0$  °C, 2 and 3 °C, respectively, greater than  $T_m$  for the peptide free lipid mixture. This trend for the  $T_m$ 's of DPPC/PG bilayers upon peptide addition indicates a greater gel-phase bilayer stability for the peptide/lipid mixtures as the phase-transition temperature of the bilayer lipid matrix is approached. The gel-to-lipid-crystalline phase-transition temperature  $T_m$  derived from the complementary  $I_{2935}/I_{2880}$  ratio for all the phospholipid/peptide mixtures are also between 2 and 3 °C greater than the  $T_m$  of the peptide-free sample. However, the widths

of the  $I_{2935}/I_{2880}$  phase transitions are greater than that of the phospholipid mixture alone, increasing slightly in the order of  $\Delta T_{\text{RL4}} \leq \Delta T_{\text{SP-B peptide}} \leq \Delta T_{\text{RL8}}$ . For the RL<sub>8</sub> lipid/peptide liposomes, the temperature profile related to lateral chain-chain interactions, as measured by the peak intensity ratio  $I_{2850}/I_{2880}$ , displays a phase-transition breadth  $\Delta T$  of  $15.0 \pm 3.5$  °C, which is considerably greater than that of either the pure lipid mixture or both of the other peptide/phospholipid dispersions. The  $I_{2850}/I_{2880}$  phase-transition width for the RL<sub>4</sub> reconstituted liposome is less than that of the pure lipid mixture, demonstrating increased lateral chain-chain cooperativity due to the peptide complexation. Marked decreases in the phase-transition cooperativities compared to the perturbant free bilayer system are manifest in the pure lateral chain-chain  $I_{2850}/I_{2880}$  and the  $I_{2935}/I_{2880}$  indices of the RL<sub>8</sub> reconstituted liposomes. In comparing the various peptide-containing bilayer dispersions at temperatures 15 °C above and below their respective  $T_m$ 's, the reconstituted complex with SP-B peptide shows generally the greatest disorder in both the gel and liquid-crystalline phases. The RL<sub>4</sub> and RL<sub>8</sub> species have nearly the same order parameters in the gel state, but the RL<sub>8</sub> system shows increased order in the liquid-crystalline phase, perhaps due to the longer stretches of hydrophobic leucines dipping through the interface region into the upper portions of the bilayer. In this manner the leucines act as

"spacers" between the intrinsically more disordered liquid-crystalline bilayer lipids.

## DISCUSSION

The thermotropic behavior of the reconstituted multilamellar lipid dispersions of a 3:1 phospholipid mixture of dipalmitoylphosphatidylcholine and phosphatidylglycerol with pulmonary surfactant related peptides show effects on the lipid bilayer order/disorder and phase-transition cooperativity properties from interactions originating from the peptide complexation. Association of residues 59–81 of SP-B and the 21 amino acid residue RL<sub>4</sub> and RL<sub>8</sub> peptides to the liposomal surface increases bilayer stability ( $T_m$  increases by 2–3 °C) but generally decreases the cooperativity of the gel-to-liquid-crystalline transitions, particularly, in terms of the order parameter monitoring simultaneously both inter- and intrachain interactions ( $I_{2935}/I_{2880}$ ). With respect to the parameter sensing pure chain-chain order/disorder characteristics ( $I_{2850}/I_{2880}$ ), only the RL<sub>8</sub> peptide/phospholipid mixture distinctly exhibits a decreased cooperativity in the bilayer melting process. Interestingly, the RL<sub>4</sub> peptide/lipid complex shows an increase in phase-transition cooperativity in terms of the interchain  $I_{2850}/I_{2880}$  index in comparison to the pure DPPC/PG binary complex but exhibits a significant decrease in cooperativity when the  $I_{2935}/I_{2880}$  indices, which probe both inter- and intrachain order/disorder properties, are examined.

The Raman spectroscopic data suggest a model for the peptide/phospholipid complex in which the hydrophilic peptides interact with the charged phosphatidylglycerol headgroup components of the bilayer to form a more constrained lipid matrix than that of the peptide-free system. The relatively ordered liquid-crystalline phases suggest that the peptide/headgroup associations have inhibited lipid lateral diffusion. These bilayer constraints probably lead to the formation of small laterally segregated domains that have an increase in PG concentration. That is, the recombinant liposomes containing the peptides with the most hydrophilic amino acids per peptide, the SP-B and RL<sub>4</sub> sequences, exhibit both increased bilayer stability, as demonstrated by an increase in  $T_m$ , and the most cooperative melting processes in terms of chain-chain correlation parameters,  $I_{2850}/I_{2880}$ . (The hydrophilic/hydrophobic residue ratios for the three peptides are about 1:1 for SP-B peptide, 1:3 for RL<sub>4</sub>, and 1:6 for RL<sub>8</sub>.)

The lipid headgroup constraints engendered by electrostatic interactions with the peptides provide a plausible rationale for the differences in phase-transition widths  $\Delta T$  values derived from the  $I_{2935}/I_{2880}$  and  $I_{2850}/I_{2880}$  parameters, respectively, for particularly the SP-B and RL<sub>4</sub> peptide/lipid complexes. That is, the  $I_{2850}/I_{2880}$  values reflect more or nearly as cooperative bilayer melting processes as the DPPC/PG liposomes, while the  $I_{2935}/I_{2880}$  parameters suggest far less cooperative melting curves than the control system. Our view is that the SP-B and RL<sub>4</sub> peptides constrain the bilayer packing to a distorted lattice arrangement. Within this deformed lipid arrangement, lattice defects could easily accommodate the formation of acyl chain gauche conformers that arise on increasing temperature. This trans/gauche isomerization process would occur over a broader temperature range than that observed in the control DPPC/PG multilayers and would be sensed by the parameter responsive to both lateral and intrachain interactions, namely, the  $I_{2935}/I_{2880}$  parameter. Since the lipid headgroup-peptide interactions are energetically comparable throughout a given bilayer domain, this constraint, affecting chain packing characteristics, would be relieved within a smaller temperature interval than that required for the trans/gauche isomerizations discussed above. It is this

lateral chain-chain behavior, sensed by the  $I_{2850}/I_{2880}$  index, that is reflected in the relatively narrow  $\Delta T$  values compared to that observed in DPPC/PG bilayers alone. In contrast, the RL<sub>8</sub> recombinant bilayer exhibits approximately the same values for  $\Delta T$  irrespective of the peak height intensity ratio used in the determination (see Table I). This behavior is consistent with the less stringent headgroup constraint placed by RL<sub>8</sub> because of the greatly reduced hydrophilic/hydrophobic peptide ratio compared to that of the RL<sub>4</sub> and SP-B systems.

In the association of the various peptides to the liposomal surface, we assume that the hydrophobic portions of the peptides remain generally in the lipid interface region, penetrating very little, if at all (except possibly for RL<sub>8</sub>), into the acyl chain region of the bilayer. If the peptide hydrophobic residues significantly disordered the hydrocarbon portion of the bilayer, then a decrease in  $T_m$  would be expected, rather than the observed increase in  $T_m$ . This peptide-lipid interaction is classified as type I, according to the scheme of Papahadjopoulos et al. (1975); that is, the bilayer interaction depends strongly on electrostatic binding and results in a small increase or no change in the  $T_m$  of the liposome.

Cochrane and Revak (1990, and unpublished observations) found that substitution of hydrophobic for hydrophilic residues in a sequence of SP-B (peptide residues 59–81), and in RL<sub>4</sub>, did not reduce the surface tension of the reconstituted synthetic surfactant in comparison to that of the peptide-free dispersion. In addition, a 21-residue peptide consisting of only arginine (poly-R), a highly hydrophilic polypeptide, when reconstituted with DPPC/PG reduced the surface tension at the air-water interface of the bubble surfactometer to a lower level than did the SP-B fragment-phospholipid surfactant. By contrast, similar peptides bearing a negatively charged aspartic acid (DL<sub>4</sub>) instead of arginine or lysine were largely inactive. In additional fluorescence investigations these authors prepared synthetic polypeptides, poly-R and RL<sub>4</sub>, which contained a single tryptophan in the center of the peptide (surrounded by two L's in the case of RL<sub>4</sub>) for reconstitution in DPPC/PG bilayers. Their results suggested that, in the RL<sub>4</sub> recombinant, tryptophan existed in a more hydrophobic environment than the tryptophan in the poly-R liposome, which was in a hydrophilic milieu. These results emphasize the importance of the electrostatic interaction between positively charged amino acids and negatively charged phospholipids in these model surfactants.

An increase in the phase-transition  $T_m$  of a model lung surfactant bilayer system has been described by Baatz et al. (1990) in which the bovine hydrophobic surfactant protein, SP-B, interacted with liposomes composed of DPPC and PG. *cis*-Parinaric acid (*cis*-PnA) and 1,6-diphenylhexa-1,3,5-triene (DPH), fluorescent probes incorporated into the DPPC/PG phospholipid bilayers, demonstrated that while  $T_m$  increased upon addition of SP-B, the lipid chain order of the bilayer interior was unaffected by the presence of the protein. The surface-sensitive phospholipid fluorescence probes, 1-acyl-2-[N-(7-nitro-2-benzoxa-1,3-diazol-4-yl)amino]hexanoyl]-phosphatidylglycerol (6-NBD-PG) and the analogous phosphatidylcholine compound (6-NBD-PC), indicated that SP-B induced bilayer surface order through a putative interaction with the charged PG headgroups.

In contrast to the effects of SP-B surfactant protein on model bilayer assemblies, a deuterium NMR study by Simatos et al. (1990) of dimyristoylphosphatidylcholine-*d*<sub>54</sub> multilamellar vesicles reconstituted with the hydrophobic porcine surfactant fraction SP-C indicated that the incorporation of

8% (w/w) protein into the bilayer lowered the  $T_m$  by 2.5 °C. In addition, the SP-C enhanced the rate of adsorption of the DMPC at air-water interfaces. In separate studies, Cochrane and Revak (unpublished observations) found that lipid systems containing SP-C did not reduce the surface tension measured by the bubble surfactometer in comparison to systems containing SP-B.

In summary, the interactions of a portion of the human surfactant SP-B (residues 59–81) and analogous peptides, RL<sub>4</sub> and RL<sub>8</sub>, with DPPC/PG mixtures induce more stable gel phases than the peptide-free bilayers, a finding consistent with the interaction of the entire bovine surfactant protein SP-B with DPPC/PG bilayers (Batz et al., 1990). The SP-B peptide and the RL<sub>4</sub> and RL<sub>8</sub> derivatives effectively stabilize the DPPC/PG bilayer assembly through electrostatic head-group constraints; that is, the positively charged peptide moieties interact with the PG headgroups. The headgroups in turn are connected by hydrophobic tethers. As judged by gel and lipid-crystalline phase order parameters, the RL<sub>4</sub> and RL<sub>8</sub> peptides appear more effective in increasing liquid-crystalline order than the SP-B derivative. However, the main phase-transition temperature  $T_m$  is increased by approximately the same amount for the DPPC/PG liposomes containing either the RL<sub>4</sub>, RL<sub>8</sub>, or SP-B fragments. The corresponding cooperativities of the various phase transitions for the three model surfactant systems, determined by the  $I_{2935}/I_{2880}$  parameter, which is sensitive both to interchain interactions and trans/gauche isomerizations, are decreased compared to the control lipid bilayer. For the three reconstituted lipid/peptide liposomes, the vibrational probe monitoring pure chain-chain interactions ( $I_{2850}/I_{2880}$ ) shows an increase in the order of the liquid-crystalline phases. Reflecting the phase-transition cooperativities,  $\Delta T$  determined from the  $I_{2850}/I_{2880}$  parameter is only increased for the lipid/RL<sub>8</sub> bilayer complex. Interaction with the peptides also reduces the variations in bilayer packing arrangements that lead to changes in integrated band intensities when the complex is examined as a function of temperature. The composite behavior of the DPPC/PG liposomes reconstituted with any one of the three polypeptides, SP-B residues 59–81, RL<sub>4</sub>, or RL<sub>8</sub>, suggests that the order induced by the constraints resulting from the interaction of the charged amino acid residues with the PG headgroups may be important features of a functionally successful lung surfactant.

#### ACKNOWLEDGMENTS

J.S.V. and I.W.L. acknowledge valuable discussions with Drs. Ralph Adams and Neil Lewis regarding various aspects of this work and thank Dr. Sherwin Straus for introducing us to the interesting area of pulmonary surfactants. Mr. John Powell of the NIH DCRT was of considerable help in the data analysis and graphical renditions.

#### REFERENCES

- Batz, J. E., Elledge, B., & Whitsett, J. A. (1990) *Biochemistry* 29, 6714–6720.
- Clements, J. A. (1977) *Am. Rev. Respir. Dis.* 115, 67–71.
- Cochrane, C. G., & Revak, S. D. (1990) *Pediatr. Res.* 27, 297A.
- Dluhy, R. A., Reilly, K. E., Hunt, R. D., Mitchell, M. L., Mautone, A. J., & Mendelsohn, R. (1989) *Biophys. J.* 56, 1173–1181.
- Enhörning, G. (1977) *J. Appl. Physiol.* 43, 198–203.
- Flory, P. J. (1969) *Statistical Mechanics of Chain Molecules*, Interscience, New York.
- Glasser, S. W., Korfhagen, T. R., Weaver, T., Pilot-Matias, T., Fox, J. L., & Whitsett, J. A. (1987) *Proc. Natl. Acad. Sci. U.S.A.* 84, 4007–4011.
- Harwood, J. L., & Richards, R. J. (1985) *Mol. Aspects Med.* 8, 423–514.
- Hawgood, S., Benson, B. J., Schilling, J., Damm, D., Clements, J. A., & White, R. T. (1987) *Proc. Natl. Acad. Sci. U.S.A.* 84, 66–70.
- Hill, I. R., & Levin, I. W. (1979) *J. Chem. Phys.* 70, 842–851.
- Jacobs, K. A., Phelps, D. S., Steinbrink, R., Fisch, J., Kriz, R., Mitsock, L., Dougherty, J. P., Taeusch, H. W., & Floros, J. (1987) *J. Biol. Chem.* 262, 9808–9811.
- King, R. J., Klass, D. J., Gikas, E. G., & Clements, J. A. (1973) *Am. J. Physiol.* 224, 788–795.
- Kirchhoff, W. H., & Levin, I. W. (1987) *J. Res. Natl. Bur. Stand. (U.S.)* 92, 113–128.
- Lavialle, F., & Levin, I. W. (1980) *Biochemistry* 19, 6044–6050.
- Levin, I. W. (1984) *Adv. Raman Spectrosc.* 11, 1–49.
- Levin, I. W. (1985) *Chemical, Biological and Industrial Applications of Infrared Spectroscopy* (Durig, J. R., Ed.) pp 173–197, John Wiley and Sons, New York.
- Mautone, A. J., Reilly, K. E., & Mendelsohn, R. (1987) *Biochim. Biophys. Acta* 896, 1–10.
- Merrifield, R. B. (1963) *J. Am. Chem. Soc.* 85, 2149–2154.
- Papahadjopoulos, D., Moscarello, M., Eylar, E. H., & Isac, T. (1975) *Biochim. Biophys. Acta* 401, 317–335.
- Phizackerley, P. J. R., Town, M. H., & Newman, G. E. (1979) *Biochem. J.* 183, 731–736.
- Reilly, K. E., Mautone, A. J., & Mendelsohn, R. (1989) *Biochemistry* 28, 7368–7373.
- Revak, S. D., Merritt, T. A., Hallman, M., & Cochrane, C. G. (1986) *Am. Rev. Respir. Dis.* 134, 1258–1265.
- Revak, S. D., Merritt, T. A., Degryse, E., Stefani, L., Courtney, M., Hallman, M., & Cochrane, C. G. (1988) *J. Clin. Invest.* 81, 826–833.
- Revak, S. D., Merritt, T. A., Hallman, M., Heldt, G., La Polla, R. J., Hoey, K., Houghten, R. A., & Cochrane, C. G. (1991) *J. Pediatr. Res.* (in press).
- Scarpelli, E. M. (1988) *Surfactants and the Lining of the Lung*, Johns Hopkins Press, Baltimore, MD.
- Seelig, A., & Seelig, J. (1977) *Biochemistry* 16, 47–51.
- Simatos, G. A., Forward, K. B., Morrow, M. R., & Keough, K. M. W. (1990) *Biochemistry* 29, 5807–5814.
- Suzuki, Y., Curstedt, T., Grossman, G., Kobayashi, T., Nilsson, R., Nohara, K., & Robertson, B. (1986) *Eur. J. Respir. Dis.* 69, 336–345.
- Takahashi, A., & Fujiwara, R. (1986) *Biochem. Biophys. Res. Commun.* 135, 527–532.
- Warr, R. G., Hawgood, S., Buckley, D. I., Crisp, T. M., Schilling, J., Benson, B. J., Ballard, P. L., Clements, J. A., & White, R. T. (1987) *Proc. Natl. Acad. Sci. U.S.A.* 84, 7915–7919.
- Whitsett, J. A., Ohning, B. L., Ross, G., Meuth, J., Weaver, T., Holm, B. A., Shapiro, D. L., & Notter, R. H. (1986) *Pediatr. Res.* 20, 460–467.